arXiv:1204.0360v2 [hep-th] 23 Oct 2012

Nordita-2012-28
RH-03-2012

Thermal Correlators in Holographic Models with Lifshitz scaling

Ville Keränen,[1,2] [*], **Larus Thorlacius,**[1,2] [†]

[1] *Nordita*
KTH Royal Institute of Technology and Stockholm University
Roslagstullsbacken 23, SE-106 91 Stockholm, Sweden

[2] *University of Iceland, Science Institute*
Dunhaga 3, IS-107 Reykjavik, Iceland

Abstract

We study finite temperature effects in two distinct holographic models that exhibit Lifshitz scaling, looking to identify model independent features in the dual strong coupling physics. We consider the thermodynamics of black branes and find different low-temperature behavior of the specific heat. Deformation away from criticality leads to non-trivial temperature dependence of correlation functions and we study how the characteristic length scale in the two point function of scalar operators varies as a function of temperature and deformation parameters.

1 Introduction

A number of holographic models have been introduced to study quantum critical systems in low dimensions, see [1–5] for reviews. In the holographic approach, relatively simple classical or semi-classical calculations are carried out in a suitably chosen gravitational background and the results interpreted in terms of strongly coupled physics in the dual field theory. For condensed matter applications, the holographic models

---

[*] vkeranen@nordita.org
[†] larus@nordita.org

are usually of the bottom up variety, where key symmetries and conserved charges of the dual system under study are realized by coupling gravity to a minimal number of additional fields. Without the benefit of extended supersymmetry and the pedigree of a consistent embedding into string theory, the validity of the gauge theory/gravity correspondence is very much an open question for bottom up models. On the other hand, they offer a simple phenomenological setting in which to study a range of physical effects and one hopes to identify a set of generic features in bottom up models that may also be shared by more realistic top down constructions. Much of the work in this area has focused on systems with an underlying conformal symmetry. This is partly because conformal symmetry is realized in a number of interesting physical systems, but also because the assumption of conformal symmetry often simplifies calculations. On the other hand, conformal symmetry is usually not present in condensed matter systems and generic quantum critical points exhibit scale invariance without conformal invariance.

In a quantum phase transition, the ground state of a system changes abruptly when some parameter of the system is varied through a critical value (for reviews, see *e.g.* [6, 7]). As in a conventional phase transition, characteristic length scales of the system diverge at a quantum critical point and there is an emergent scaling symmetry of the form

$$t \to \lambda^z\, t, \qquad \vec{x} \to \lambda \vec{x}, \tag{1}$$

where $z \geq 1$ is referred to as the dynamical critical exponent. For $z > 1$ the scaling at the quantum critical point is anisotropic between the temporal and spatial directions, commonly referred to as Lifshitz scaling in the literature.

In this paper we study finite temperature effects in two different bottom up holographic models that exhibit Lifshitz scaling. On the one hand we consider Einstein-Maxwell gravity coupled to a massive vector (Proca) field. We refer to this as the EMP model (for Einstein-Maxwell-Proca). It is based on a model introduced in [8] involving a pair of two- and three-form field strengths coupled to Einstein gravity with a negative cosmological constant. This was reformulated in [9] as Einstein gravity coupled to a Proca field, and in [10] a $U(1)$ Maxwell field was added in order to study dual systems at finite charge density. The second model was introduced in [11] and consists of Einstein gravity coupled to a dilaton field and a pair of $U(1)$ gauge fields. It is a generalization of an earlier model considered in [9] and will be referred to below as the EDM model (for Einstein-Dilaton-Maxwell). A motivation for studying two models at once is to get a handle on how much of the physics is controlled by the anisotropic scaling invariance (1) and how much is model dependent.

We compare charged black brane solutions and some of their thermodynamics between the two models. We then consider two point correlation functions of operators dual to a probe scalar field in these holographic models. The two point correlators exhibit screening at finite temperature and we obtain the dependence of the screening length on temperature and deformation parameters in the two holographic models. These results can be compared at a qualitative level to corresponding computations at weak coupling. In particular, the quantum Lifshitz model provides a well controlled theoretical setting to study thermal effects near a $z = 2$ fixed point [12–14]. The temperature dependence of characteristic length scales was studied via the two point function of a scaling operator in this model in [15]. It was found that the two point correlation function at spatially separated points vanishes at finite temperature due to an infrared divergence. This makes the system very sensitive to deformations away from the critical point. The authors of [15] considered the effect on the two point function of introducing an irrelevant operator and found that it restores correlations between spacelike separated points and introduces a temperature dependent characteristic length scale into the two point function.

In general, heating up a system at a quantum critical point introduces a length scale that breaks the scaling symmetry, but at the same time it broadens the region in parameter space that is controlled by the underlying scale invariant theory. In an otherwise scaling symmetric theory, the dependence of a characteristic length scale ξ on temperature is given by

$$\xi = cT^{-1/z}, \tag{2}$$

where c is some constant numerical coefficient. As one deforms the system away from the critical point, the temperature dependence of the characteristic length scale becomes more generic. Consider a set of deformation parameters λ_i, which for convenience are defined so that they have dimensions of inverse length. At zero temperature $\lambda_i = 0$ corresponds to infinite correlation length. Away from $\lambda_i = 0$, the temperature dependence becomes

$$\xi = T^{-1/z}\eta(T^{-1/z}\lambda_i), \tag{3}$$

where η is some generic function of its arguments. The only requirement is that $\eta(0) = c$.

In the holographic models, turning on a finite temperature leads to the exponential decay of two point correlation functions between spacelike separated points, with a temperature dependent correlation length ξ. If the finite temperature is the only deformation parameter, then the temperature dependence of the correlation length will be of the simple form (2). More interesting behavior is seen if we consider deformations away from the fixed point. We study two different types of relevant deformations of the model. The first one is to turn on a chemical potential for a conserved $U(1)$ charge,

$$S_1 = \int d\mathbf{x}d\tau\mu\rho, \tag{4}$$

which on the gravity side corresponds to considering gravitational solutions with an electric flux. The relevant black brane solutions in the EMP model were constructed in [10] and in the EDM model in [11]. As the temperature is lowered, this deformation will take the system from the Lifshitz fixed point to a "locally critical" fixed point corresponding to the appearance of an $AdS_2 \times R^2$ region in the spacetime.

The second type of deformation we consider is to add a double trace deformation for the probe scalar field

$$S_2 = \int d\mathbf{x} d\tau \lambda \mathcal{O}^2, \tag{5}$$

whose correlation functions we are interested in. This deformation is less dramatic than the previous one in that, as the temperature is lowered, the theory flows to another Lifshitz symmetric fixed point.

The paper is organized as follows. In section 2 we briefly review the calculation of the finite temperature correlation function in the quantum Lifshitz model in [15]. In section 3 we introduce the two holographic models with Lifshitz scaling and review properties of their charged black brane solutions. In section 4 we compare some thermodynamic properties of black branes and conclude that the low temperature physics differs between the two models. In section 5 we obtain two point correlation functions in a charged black brane background. We first consider operators of large scaling dimensions, for which the two point correlator can be obtained in a geodesic approximation, and then repeat the analysis for operators of general scaling dimensions. In section 6 we calculate the two point correlation function with a double trace deformation at finite temperature (and at a vanishing charge density). Finally in section 7 we summarize our results.

2 Thermal correlators in the quantum Lifshitz model

A free field theory realization of a class of $z = 2$ quantum critical points is provided by the quantum Lifshitz model,

$$S_0 = \frac{1}{2} \int d^2x d\tau \Big((\partial_\tau \chi)^2 + K(\nabla^2 \chi)^2 \Big). \tag{6}$$

Here we will briefly review the finite temperature correlation functions in this model, obtained in [15], in order to compare them to the results of holographic calculations later in the paper. We refer to [12–14] for more detailed discussions of the quantum Lifshitz model.

The operators of interest are the so called monopole operators[1]

$$\mathcal{O}(x) = e^{2\pi i \chi(x)}. \tag{7}$$

The vacuum two point correlation function has the scaling form

$$G(\mathbf{x}, \mathbf{x}') = \langle \mathcal{O}(\mathbf{x}, 0) \mathcal{O}(\mathbf{x}', 0) \rangle \propto \frac{1}{|\mathbf{x} - \mathbf{x}'|^{\pi/\sqrt{K}}}, \tag{8}$$

---

[1] The name monopole operator comes from a dual gauge theory representation of the same model, where one has $E_i = \epsilon_{ij} \partial_j \chi$. The operator in (7) creates a monopole in the dual gauge field [15].

which follows from logarithmic correlations of χ. At finite temperature the contribution from the zeroth Matsubara mode to the χ correlator is proportional to

$$T\int d^2k\frac{1-e^{i\mathbf{k}\cdot(\mathbf{x}-\mathbf{x}')}}{K\mathbf{k}^4}, \tag{9}$$

where the momentum integral is seen to diverge logarithmically with an infrared cutoff L. The two point correlation function of spacelike separated monopole operators thus vanishes at finite temperature in the infinite volume limit,

$$G(\mathbf{x},\mathbf{x}')\propto\frac{1}{|\mathbf{x}-\mathbf{x}'|^{\pi/\sqrt{K}}}e^{-\frac{\pi T}{2K}|\mathbf{x}-\mathbf{x}'|^2\log L}\to 0. \tag{10}$$

Spatial correlations are restored away from the scaling limit of the free theory. The authors of [15] consider a marginally irrelevant deformation of the free model, by adding an interaction term

$$S_{int}=\frac{1}{2}\int d^2x d\tau u(\nabla\chi)^4, \tag{11}$$

which corresponds to slightly moving away from the critical point. This deformation leads to a logarithmic violation of scaling symmetry, which changes the finite temperature behavior. The interaction induces a term

$$v^2(\nabla\chi)^2, \tag{12}$$

into the effective action for χ already at one loop. This term changes the low momentum behavior of the theory dramatically and cures the infrared divergences. By using a large N gap equation the authors of [15] find

$$v^2\approx 4T\sqrt{K}\frac{\log\Big(-\log T\Big)}{-\log T}, \tag{13}$$

which is understood to hold for small T. This means that there is a non-trivial (temperature dependent) length scale induced in the theory

$$\xi_T^2=\frac{K}{v^2}. \tag{14}$$

Using the new effective action leads to a two point correlator of monopole operators of the following form:

$$G(\mathbf{x},\mathbf{x}')\propto\exp\left[-\frac{\pi T}{2v^2}\frac{|\mathbf{x}-\mathbf{x}'|^2}{\xi_T^2}\left(\log\left[\frac{2\xi_T}{|\mathbf{x}-\mathbf{x}'|}\right]+c\right)\right], \tag{15}$$

where c is a constant, for distances smaller than ξ_T, and

$$G(\mathbf{x},\mathbf{x}')\propto\exp\left[-\frac{2\pi T}{v^2}\log\left(\frac{|\mathbf{x}-\mathbf{x}'|}{\xi_T}\right)\right], \tag{16}$$

for distances larger than ξ_T. Furthermore, if one allows for vortices (spinons) in the χ field, the correlation function changes qualitatively at very large distances. Assuming a vortex energy gap E_c, one finds that correlations are exponentially decaying on a length scale $\xi_{vortex} \propto e^{E_c/2T}$ due to a vortex plasma [15].

To summarize, the authors of [15] find a non-trivial temperature dependence in correlation functions of spatially separated monopole operators, which arises on the one hand from the Lifshitz scaling region (at short distances) and on the other hand from deformations away from criticality. It seems likely that many of the details depend on the specific theory and the specific deformations that were considered in [15]. In sections 5 and 6 below, we calculate two point correlation functions of scaling operators in holographic models exhibiting Lifshitz scaling. We also find a temperature dependent thermal length scale which can be compared to that of the quantum Lifshitz model. Since the holographic models are dual to strongly coupled theories and the quantum Lifshitz model is a free field theory, one does not expect to reproduce the results of [15] in detail but rather look whether the holographic models exhibit similar trends.

3 Holographic models with Lifshitz scaling

We will consider two different holographic models, both of which realize anisotropic scaling of the form (1) through spacetime geometries that are asymptotic to the so-called Lifshitz geometry [8, 16],

$$ds^2 = \ell^2 \left(-r^{2z} dt^2 + \frac{dr^2}{r^2} + r^2 d\mathbf{x}^2 \right). \tag{17}$$

Here ℓ is a characteristic length scale of the geometry and the r, t, and $\vec{x}$ coordinates have no length dimensions. The Lifshitz metric is invariant under the transformation

$$t \to \lambda^z t, \qquad \vec{x} \to \lambda \vec{x}, \qquad r \to \frac{r}{\lambda}, \tag{18}$$

which incorporates the scaling in (1) on the t and $\vec{x}$ coordinates, while the radial coordinate r of the bulk geometry scales inversely with λ. In the rest of the paper the characteristic length will be set to $\ell = 1$. It can be re-introduced via dimensional analysis if needed. For concreteness, we will take the bulk spacetime to be 3+1 dimensional, but our results generalize in a straightforward fashion to other dimensions.

The two models both involve Einstein-Maxwell gravity with a negative cosmological constant but the asymptotic Lifshitz behavior is achieved by coupling to different matter sectors. Both models have charged black brane solutions that are asymptotic to the Lifshitz geometry and are interpreted as holographic duals of field theory configurations at finite temperature and finite charge density. The black brane geometries are not the same in the two models. In particular, their near-extremal limits differ and this has consequences for low-temperature physics in the corresponding dual field theories. One of the aims of this paper is to compare predictions for physical observables at finite temperature and explore to what extent they are model dependent.

3.1 Einstein-Maxwell-Proca theory

The first model we consider is a modified version of the holographic model first considered in [8]. In the original version, anisotropic scaling of the form (18) was obtained by coupling Einstein gravity to a pair of two- and three-form field strengths. As was shown in [9], this can be rewritten as a single massive vector field coupled to gravity and we find this formulation more convenient to work with. Finally, following [10], we include a Maxwell gauge field which is coupled to the gravitational field but not directly to the auxiliary massive vector field,

$$S_{\mathrm{EMP}} = \int \mathrm{d}^4x\sqrt{-g}\,\left(R - 2\Lambda - \frac{1}{4}F_{\mu\nu}F^{\mu\nu} - \frac{1}{4}\mathcal{F}_{\mu\nu}\mathcal{F}^{\mu\nu} - \frac{c^2}{2}\mathcal{A}_\mu\mathcal{A}^\mu\right). \tag{19}$$

The role of the massive vector field background is to modify the asymptotic behavior of the metric. One could in principle include direct couplings between the massive vector and the Maxwell gauge field, in which case having a massive vector background field would also influence the gauge field dynamics, but for simplicity we have chosen not to do that. In what follows we will refer to this theory as the EMP model.

The Lifshitz metric (17) is a solution of the equations of motion when the constants in the model are related to the dynamical critical exponent z through

$$\Lambda = -\frac{1}{2}(z^2 + z + 4), \qquad c = \sqrt{2z}, \tag{20}$$

and the massive vector field has a non-vanishing background value,

$$\mathcal{A}_t = \sqrt{\frac{2(z-1)}{z}}r^z\,, \qquad \mathcal{A}_{x_i} = \mathcal{A}_r = 0\,. \tag{21}$$

The field equations of the EMP model have been studied extensively by many authors (see [17] for a brief review) and we will not repeat the analysis here. For generic values of the dynamical critical exponent, there are no known analytic solutions describing black holes or black branes[2] but numerical solutions can easily be found using similar techniques as introduced in [19]. Below, we will present results obtained from numerical solutions of the EMP model and compare them with results obtained using analytic black brane solutions from the other model.

---

[2] An exact solution exists for $z = 4$ (or more generally $z = 2d$ where d is the number of transverse spatial dimensions) and a particular value of the electric charge on the black hole, or charge density on the black brane [10, 18].

3.2 Einstein-Dilaton-Maxwell theory

The second model is an Einstein-Dilaton-Maxwell (EDM) theory

$$S_{\mathrm{EDM}} = \int \mathrm{d}^4x\sqrt{-g}\,\left[R - 2\Lambda - \frac{1}{2}\partial_\mu\phi\partial^\mu\phi - \frac{1}{4}\sum_{i=1}^{2} e^{\lambda_i\phi}F^{(i)}_{\mu\nu}F^{(i)\mu\nu}\right]. \tag{22}$$

Models of this type were introduced in the context of non-relativistic holography in [9] and black brane solutions of this particular action were found in [11]. Dynamical solutions describing infalling energy were constructed in [20] and used to study thermalization following a non-relativistic holographic quench but here we will only consider static solutions.

The equations of motion are

$$\begin{aligned} R_{\mu\nu} - \frac{1}{2}Rg_{\mu\nu} + \Lambda g_{\mu\nu} &= T^{\phi}_{\mu\nu} + T^{(1)}_{\mu\nu} + T^{(2)}_{\mu\nu}, && (23)\\ \nabla^2\phi - \sum_{i=1}^{2}\frac{\lambda_i}{4}e^{\lambda_i\phi}F^{(i)}_{\mu\nu}F^{(i)\mu\nu} &= 0, && (24)\\ \nabla_\mu\left(e^{\lambda_i\phi}F^{(i)\mu\nu}\right) &= 0, \qquad i = 1,2\,, && (25)\end{aligned}$$

with

$$\begin{aligned} T^{\phi}_{\mu\nu} &= \frac{1}{2}\partial_\mu\phi\partial_\nu\phi - \frac{1}{4}g_{\mu\nu}(\partial\phi)^2, && (26)\\ T^{(i)}_{\mu\nu} &= \frac{e^{\lambda_i\phi}}{2}\left[F^{(i)}_{\mu\sigma}F^{(i)\,\sigma}_{\nu} - \frac{1}{4}g_{\mu\nu}F^{(i)}_{\sigma\rho}F^{(i)\sigma\rho}\right]. && (27)\end{aligned}$$

Remarkably, these field equations can be solved analytically to obtain charged black branes in asymptotically Lifshitz spacetime for any value of the dynamical critical exponent z. Below we reproduce the static black brane solutions of [11] and review some of their thermodynamic properties. We then use them to calculate finite temperature correlation functions of scalar operators in the dual field theory. At each stage, we compare our results to corresponding calculations in the EMP model.

3.2.1 Asymptotically Lifshitz solutions

We use the following metric ansatz for static solutions,

$$ds^2 = -r^{2z}f(r)dt^2 + \frac{dr^2}{r^2g(r)} + r^2(dx^2+dy^2), \tag{28}$$

for which the field equations (25) for the gauge fields are solved by

$$F^{(i)}_{rt} = \rho_i\, r_0^{z-1}\left(\frac{r}{r_0}\right)^{z-3}\sqrt{\frac{f(r)}{g(r)}}\,e^{-\lambda_i\phi(r)}, \tag{29}$$

where r_0 is an arbitrary reference value of the radial variable and the ρ_i are dimensionless constants. Under the coordinate rescaling (18), r_0 transforms like r while ρ_i remain invariant. Later on, when we consider black hole solutions it will be convenient to take r_0 as the radial location of the event horizon.

The Einstein equations (23) reduce to a pair of first order differential equations,

$$\begin{aligned} \frac{rf'}{f} - \frac{rg'}{g} &= -2(z-1) + \frac{1}{2}(r\phi')^2, && (30) \\ \frac{rf'}{f} + \frac{rg'}{g} &= -2(z+2) - \frac{1}{g}\left[2\Lambda + \frac{1}{2}\left(\frac{r_0}{r}\right)^4 \left(\rho_1^2 e^{-\lambda_1\phi} + \rho_2^2 e^{-\lambda_2\phi}\right)\right], && (31) \end{aligned}$$

and the dilaton equation (24) becomes

$$r^2\phi'' + \left[\frac{r}{2}\frac{f'}{f} + \frac{r}{2}\frac{g'}{g} + z - 3\right] r\phi' + \frac{1}{2g}\left(\frac{r_0}{r}\right)^4 \left(\lambda_1\rho_1^2 e^{-\lambda_1\phi} + \lambda_2\rho_2^2 e^{-\lambda_2\phi}\right) = 0. \qquad (32)$$

The Lifshitz geometry (17) has $f(r) = g(r) = 1$, for which equation (30) is solved by $e^\phi = \mu r^{2\sqrt{z-1}}$. The integration constant μ can be rescaled by using a symmetry of the field equations under a constant shift of ϕ accompanied by a compensating rescaling of the ρ_i, and we find it convenient to normalize it as follows,

$$e^\phi = \left(\frac{r}{r_0}\right)^{2\sqrt{z-1}}, \qquad (33)$$

or equivalently set $\mu\, r_0^{2\sqrt{z-1}} = 1$. To determine the parameters of the Lifshitz background we insert this into the remaining field equations and set $\rho_2 = 0$. From the dilaton equation (32) we obtain

$$2(z+2)\sqrt{z-1} = -\frac{\lambda_1\rho_1^2}{2}\left(\frac{r_0}{r}\right)^{4+2\sqrt{z-1}\lambda_1}, \qquad (34)$$

which requires

$$\lambda_1 = -\frac{2}{\sqrt{z-1}}, \qquad \rho_1 = \sqrt{2(z-1)(z+2)}, \qquad (35)$$

and equation (31) then relates the cosmological constant to the dynamical critical exponent,

$$\Lambda = -\frac{1}{2}(z+1)(z+2). \qquad (36)$$

We note that λ_1 is negative. The sign of λ_i in (22) determines how the coupling of the corresponding gauge field changes with radial location and with the dilaton profile in (33) we find that $F^{(1)}_{\mu\nu}$ is strongly coupled in the asymptotic $r \to \infty$ region. This makes the model less satisfactory, but it is not a serious problem as long as $F^{(1)}_{\mu\nu}$ does not couple directly to anything outside the gravitational sector. Its only role should be to modify the asymptotic behavior of the metric from AdS to Lifshitz through the gravitational back reaction to its background value. For applications, such as holographic superconductors or fermion spectral densities, any additional matter fields in the model should only be charged under $F^{(2)}_{\mu\nu}$ and not under $F^{(1)}_{\mu\nu}$.

3.2.2 Charged black branes in EDM model

The charged black brane solutions in [11] have $f = g$ and the same dilaton profile (33) as in the purely Lifshitz background. The Einstein equation (31) then reduces to

$$r g' + (z+2)(g-1) = -\frac{\rho_2^2}{4}\left(\frac{r_0}{r}\right)^{4+2\sqrt{z-1}\lambda_2}, \tag{37}$$

while the dilaton equation (32) is satisfied if

$$r g' + (z+2)(g-1) = -\frac{\lambda_2 \rho_2^2}{4\sqrt{z-1}}\left(\frac{r_0}{r}\right)^{4+2\sqrt{z-1}\lambda_2}. \tag{38}$$

It follows that $\lambda_2 = \sqrt{z-1}$ and the solution for a charged black brane with an event horizon at $r = r_0$ is given by

$$f(r) = g(r) = 1 - \left(1+\frac{\rho_2^2}{4z}\right)\left(\frac{r_0}{r}\right)^{z+2} + \frac{\rho_2^2}{4z}\left(\frac{r_0}{r}\right)^{2z+2}, \tag{39}$$

$$F^{(1)}_{rt} = \sqrt{2(z-1)(z+2)}\, r_0^{z-1}\left(\frac{r}{r_0}\right)^{z+1}, \tag{40}$$

$$F^{(2)}_{rt} = \rho_2\, r_0^{z-1}\left(\frac{r_0}{r}\right)^{z+1}, \tag{41}$$

$$e^{\phi} = \left(\frac{r}{r_0}\right)^{2\sqrt{z-1}}, \tag{42}$$

This solution is valid for any value of $z \geq 1$ and can be generalized in a straightforward fashion to more general spacetime dimensions [11]. In the $z \to 1$ limit, the metric and the Maxwell gauge field $F^{(2)}_{rt}$ reduce to those of a standard AdS-Reissner-Nordström black brane, while the auxilliary gauge field $F^{(1)}_{rt}$ vanishes and the dilaton becomes independent of r.

The scale transformation (18) is a symmetry of the black brane metric (39), provided r_0 is rescaled in the same way as r. This is a special feature of black branes with a planar horizon and it implies that the radial location of the horizon r_0 does not have any physical meaning by itself. The same is true for planar black branes in the EMP model. It is therefore important to always use scale invariant combinations of physical quantities when presenting results obtained in these holographic models.

3.2.3 Asymptotic behavior

A distinctive feature of numerical black brane solutions in the EMP model is the presence of a mode that is not well behaved in the $r \to \infty$ asymptotic region [19,21,22]. Depending on the value of the dynamical critical exponent, it can either be a growing mode that takes the system away from the Lifshitz fixed point or a decaying mode that only converges very slowly to the asymptotic fixed point. The solutions are usually obtained by numerically integrating the field equations of the model, starting from initial conditions near the horizon and proceeding out towards the asymptotic region. The initial data at the horizon is then fine tuned to remove the mode in question. This works reasonably well over a range of black brane temperature and charge density but the required fine tuning becomes progressively more difficult as the temperature is lowered and the black brane charge approaches its extremal value.

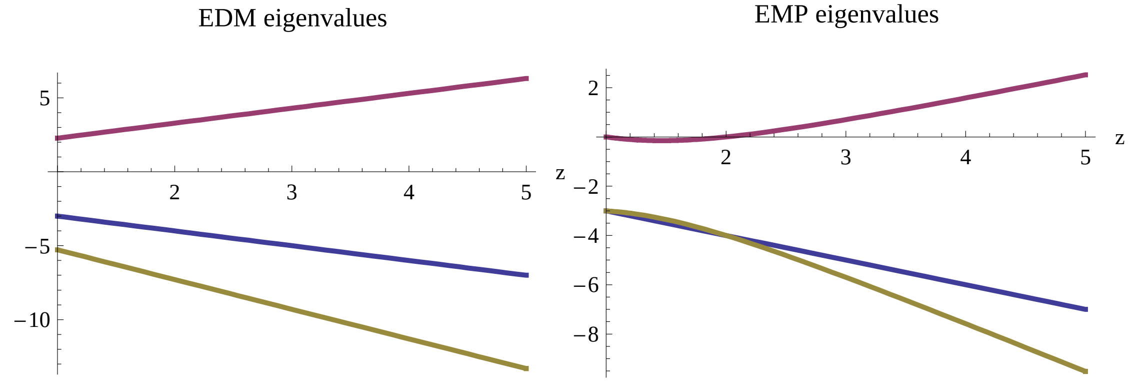

Figure 1: A comparison of mode eigenvalues of the linearized field equations around a Lifshitz background in the EDM model (left) and the EMP model (right).

In the large r limit, the analytic black brane solutions of the EDM model have modes that go as r^{-z-2} and r^{-2z-2}, and the accompanying coefficients are the brane energy density and the charge density respectively. It turns out, however, that the Lifshitz fixed point is always unstable in this model and that a generic perturbation around it will include a growing mode that is not present in the black brane solutions. To see this, we linearize the field equations (30) - (32) around the Lifshitz fixed point. The function $f(r)$ can be eliminated between the two Einstein equations, leaving a system involving only $g(r)$ and $\phi(r)$. We allow for a dilaton that varies from its background value,

$$e^{\phi(r)} = \left(\frac{r}{r_0}\right)^{2\sqrt{z-1}} e^{\sqrt{z-1}\,\varphi(r)}, \tag{43}$$

and write $g(r) \approx 1 + \gamma(r)$. Working to first order in $\gamma(r)$, $\varphi(r)$, and $\chi(r) \equiv r\varphi'(r)$, we obtain

$$r\frac{d}{dr}\begin{bmatrix}\gamma\\ \varphi\\ \chi\end{bmatrix} = \begin{bmatrix}-z-2 & -(z-1)(z+2) & -z+1\\ 0 & 0 & 1\\ 0 & 2(z+1)(z+2) & -z-2\end{bmatrix}\begin{bmatrix}\gamma\\ \varphi\\ \chi\end{bmatrix} - \frac{\rho_2^2}{4}\left(\frac{r_0}{r}\right)^{2z+2}\begin{bmatrix}1\\ 0\\ 0\end{bmatrix}, \tag{44}$$

At large r, a solution to the full non-linear system will approach a linear combination of the eigenmodes of the linearized system plus a universal mode coming from the source term. The eigenvalues,

$$-z-2, \quad \frac{1}{2}\left(-z-2 \pm \sqrt{(z+2)(9z+10)}\right), \tag{45}$$

are plotted on the left in Figure 1, showing that the system has a growing mode for any value of z. The result of the corresponding mode analysis of the EMP model [21] is shown on the right in the figure, for comparison. In both models, turning on a growing mode would change the asymptotic behavior of the metric and take the dual field theory away from the Lifshitz UV fixed point. In this paper we are interested in models with Lifshitz scaling and we therefore only consider configurations where the growing mode is not turned on.

Both models have an eigenmode that falls off as r^{-z-2} and from a general analysis of holographic renormalization in asymptotically Lifshitz spacetime [23–27] one concludes that the coefficient in front of such a mode is proportional to the energy density of the configuration. In both models the brane electric charge density enters the linearized system as a universal mode due to a source term but the falloff with r is different. In the EMP model the charge mode falls off as r^{-4}, independent of z, while in the EDM model the falloff is r^{-2z-2} and at leading order this mode only enters in the metric function and not in the dilaton field.

3.2.4 Extremal Lifshitz black branes

At the extremal value of the charge density, $\rho_2 = \pm\sqrt{4(z+2)}$, the metric function (39) in the EDM model has a double zero at the horizon,

$$f(r) \approx (z+1)(z+2)\left(\frac{r}{r_0}-1\right)^2 \tag{46}$$

and the near horizon metric can be written in $\mathrm{AdS}_2 \times \mathrm{R}_2$ form,

$$ds^2 \approx -\frac{1}{(z+1)(z+2)}\left[-v^2 d\hat{t}^2 + \frac{dv^2}{v^2}\right] + d\hat{x}^2 + d\hat{y}^2, \tag{47}$$

where

$$v = \frac{r}{r_0} - 1, \quad \hat{t} = (z+1)(z+2)r_0^z\, t, \quad \hat{x} = r_0\, x, \quad \text{and} \quad \hat{y} = r_0\, y. \tag{48}$$

This means that the geometry of extremal Lifshitz black branes in the EDM model is qualitatively similar to that of an extremal AdS-Reissner-Nordström black brane at $z = 1$. It follows that various holographic computations that have been performed in AdS-RN backgrounds will carry over to the EDM model in a straightforward fashion. In particular, the single fermion spectral function for probe fermions can be evaluated using similar techniques as have been used in asymptotically AdS spacetime [28–30] and we expect qualitatively similar results, including signals of non Fermi liquid behavior, to be obtained in the EDM model[3].

Less is known about extremal black branes in the EMP model. The commonly used method for finding numerical black brane solutions breaks down before the extremal limit is reached and the known exact solution at $z = 4$ is non-extremal. An analysis of the field equations of the EMP model at extremal charge density suggests that the near horizon geometry of an extremal black brane is in fact $\mathrm{AdS}_2 \times \mathrm{R}_2$ in this model as well. The near horizon metric can be brought into the same form as (47), but in this case the required coordinate transformation turns out to be non-analytic at $r = r_0$ and the Proca field also goes to zero in a non-analytic fashion at $r = r_0$.

---

[3] For calculations of fermion correlation functions in Lifshitz backrounds see [31–33].

4 Black brane thermodynamics

The Hawking temperature of an asymptotically Lifshitz black brane is determined in the usual way by considering the near horizon behavior of the metric,

$$T = \frac{r_0^{z+1}}{4\pi} \sqrt{f'(r_0) g'(r_0)}. \tag{49}$$

For the analytic black brane solutions of the EDM model one finds

$$T = \frac{r_0^z}{4\pi} \left[z + 2 - \frac{\rho_2^2}{4} \right], \tag{50}$$

while, as usual, only numerical results are available for the EMP model. Figure 2 compares the Hawking temperatures of $z = 2$ black branes in the two models. Other values of z give rise to qualitatively similar graphs.

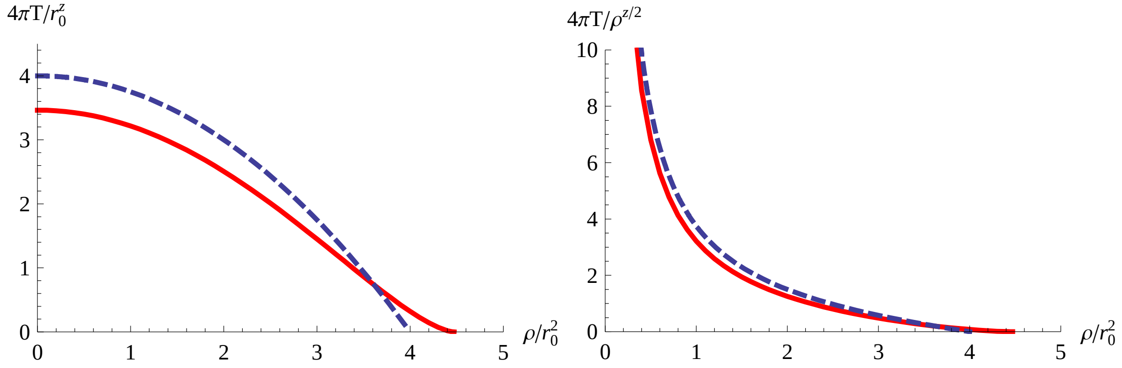

Figure 2: Hawking temperature as a function of the dimensionless charge density for $z = 2$ charged black branes. On the left, the dashed (blue) curve shows the temperature in the EDM model (equation (50)) while the solid (red) curve is from numerical solutions of the EMP model. On the right, the scale invariant combination T/ρ is shown for the same $z = 2$ data.

The EDM action (22) does not depend explicitly on the gauge potential $A_t^{(2)}$ but only its radial derivative. The associated radially conserved quantity is the charge density carried by the black brane,

$$\rho \equiv \frac{\delta S_{\mathrm{EDM}}}{\delta \partial_r A_t^{(2)}} = r^{3-z}\sqrt{\frac{g}{f}}e^{\lambda_2\phi}F_{rt}^{(2)}, \tag{51}$$

and inserting $F_{rt}^{(2)}$ and e^{ϕ} from (41) and (42) gives

$$\rho = \rho_2 r_0^2. \tag{52}$$

In the following, we have chosen to keep fixed the physical charge density ρ when calculating thermodynamic quantities and express our results in terms of scale invariant combinations such as $T/\rho^{z/2}$. An alternative choice is to instead keep fixed the chemical potential of the Maxwell field.

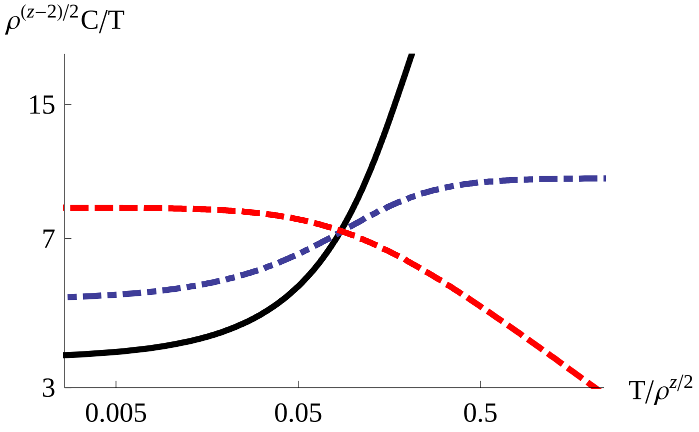

Figure 3: The ratio of specific heat to temperature in the EDM model for dynamical scaling exponents $z = 1$ (black solid), $z = 2$ (blue dot-dashed) and $z = 3$ (red dashed).

The specific heat at fixed transverse volume and charge density is easily calculated in the EDM model. It can then be compared to numerical results from the EMP model, obtained in [34], and one finds that the two models predict different low-temperature behavior for this observable. The specific heat at fixed volume and charge density in the dual boundary theory is given by

$$C_{V,\rho} = T\frac{dS}{dT}, \tag{53}$$

where $S = \pi r_0^2$ is the Bekenstein-Hawking entropy density of the black brane and the temperature T in the boundary theory is identified with the Hawking temperature (49). Keeping ρ in (52) fixed implies

$$\frac{d}{dr_0} = \frac{\partial}{\partial r_0} - \frac{2\rho_2}{r_0}\frac{\partial}{\partial \rho_2}, \tag{54}$$

and one then finds

$$\begin{aligned} \frac{C_{V,\rho}}{T} &= \frac{dS/dr_0}{dT/dr_0} \\ &= \frac{32\pi^2}{4z(z+2)-(z-4)\rho_2^2}\left(\frac{\rho}{\rho_2}\right)^{(2-z)/2}. \end{aligned} \tag{55}$$

Figure 3 plots the scale invariant combination $\rho^{(z-2)/2}C_{V,\rho}/T$ against $T/\rho^{z/2}$ for three different values of z. In all cases the C/T ratio goes to a constant at low temperature. The low temperature limit can also be seen directly by going to the extremal limit $\rho_2^2 \to 4(z+2)$ in the above expression for C/T,

$$\rho^{(z-2)/2}\,\frac{C_{V,\rho}}{T} \to 2^{z/2}(z+2)^{(z-6)/4}\pi^2 \quad \text{as} \quad T \to 0. \tag{56}$$

The low temperature behavior of the specific heat is very different in the EMP model. Numerical calculations reported in [34] show a C/T ratio at fixed charge density that grows as the temperature is lowered and diverges in the $T \to 0$ limit for all $z > 1$.

At high temperatures the specific heat in (55) satisfies a simple scaling law consistent with the underlying Lifshitz symmetry,

$$C_{V,\rho} \sim T^{2/z}. \tag{57}$$

This scaling is also seen in the EMP model [34].[4] It follows on general grounds from the statistical mechanics of a system with $\omega \sim k^z$ dispersion in two spatial dimensions [35].

5 Two point functions at finite charge density

We now turn our attention to finite temperature correlation functions. For earlier studies of scalar correlators in Lifshitz black hole backgrounds see [36, 37]. In this section we study the temperature dependence of two point correlation functions of scalar operators at fixed charge density. We first use the geodesic approximation, valid for large scaling dimensions, to simplify the calculation and get a sense of the finite temperature behavior.[5] We then consider general scaling dimensions and solve the scalar wave equation in the background spacetime of a charged Lifshitz black brane.

---

[4] The specific heat only depends on the geometry (through the entropy) and not directly on the dilaton field. More general observables, such as correlation functions of fields coupled to the dilaton, can fail to be Lifshitz symmetric because the dilaton itself transforms under a Lifshitz rescaling.

[5] The finite temperature two point function at vanishing charge density was obtained in the geodesic approximation in [20].

5.1 Geodesic approximation

First we consider operators with large scaling dimensions Δ. On the gravitational side this maps to large particle mass, for which we can approximate $m \approx \Delta$. We can use the geodesic approximation to calculate the two point function [38],

$$\langle \mathcal{O}(x)\mathcal{O}(x')\rangle \approx \epsilon^{-2\Delta} e^{-\Delta \int d\tau \sqrt{g_{\mu\nu}\frac{dx^\mu}{d\tau}\frac{dx^\nu}{d\tau}}}, \tag{58}$$

where $x^\mu(\tau)$ is the geodesic of minimal length and ϵ is an infrared cutoff in the bulk spacetime $r < 1/\epsilon$.

The metrics of interest have the form (28) and we can parametrize the geodesics as $r = r(x)$, $t = t(x)$ and $y = y(x)$, where x and y are transverse coordinates. Because of translational symmetry in the t and y directions the momenta $p_t \propto t'(x)$ and $p_y \propto y'(x)$ are conserved. By a combination of translation and rotation in the x-y plane we canalways arrange both endpoints of the geodesic to be at $y = 0$. It then follows that $y'(x) = 0$ identically, since, if the derivative did not vanish, the geodesic could not start and end at the same value of y. Similarly, for an equal time commutator, the constant value of $t'(x)$ must in fact be zero for otherwise the two endpoints would be at different values of t.

In this case, the geodesic length functional simplifies,

$$S = \Delta \int dx \sqrt{r(x)^2 + \frac{(r'(x))^2}{r(x)^2 g(r)}} \equiv \Delta \int dx L. \tag{59}$$

Since the "Lagrangian" L has no explicit x dependence, there is a conserved Hamiltonian,

$$H = \frac{\partial L}{\partial r'} r' - L = -\frac{r^2}{L}. \tag{60}$$

The value of the Hamiltonian can be calculated at the turning point of the geodesic at $r = r_*$. By translation symmetry the turning point can be taken to be at $x = 0$ and then we can use $r'(0) = 0$ to give $H = -r_*$. This way we are lead to a first order differential equation for the geodesic,

$$(r')^2 = g r^4 \left(\frac{r^2}{r_*^2} - 1\right). \tag{61}$$

The on shell particle action is now given by

$$S = \Delta \int dr \frac{L}{r'} = \frac{2\Delta}{r_*} \int_{r_*}^{\epsilon^{-1}} dr \frac{1}{\sqrt{g\left(\frac{r^2}{r_*^2} - 1\right)}}, \tag{62}$$

where we have used the chain rule and the equation of motion (61). It is straightforward to solve (61) numerically and evaluate the integral (62). Before doing this, we note that the two point function can be computed analytically for large distances. First we write (61) in integral form

$$\frac{1}{2}|\mathbf{x}-\mathbf{x}'| = \int_{r_*}^{\epsilon^{-1}} dr \frac{1}{\sqrt{gr^4\left(\frac{r^2}{r_*^2}-1\right)}}. \tag{63}$$

The key is to note that large distance $|\mathbf{x}-\mathbf{x}'|$ corresponds to a geodesic with a turning point approaching the horizon $r = r_0$. In the limit $r_* \to r_0$ the integrals (62) and (63) both diverge logarithmically at the lower end.[6] So in this limit we can approximate

$$\frac{1}{2}|\mathbf{x}-\mathbf{x}'| = \int_{r_*}^{\epsilon^{-1}} dr \frac{1}{\sqrt{gr^4\left(\frac{r^2}{r_*^2}-1\right)}} \approx \frac{1}{r_*^2}\int_{r_*} dr \frac{1}{\sqrt{g\left(\frac{r^2}{r_*^2}-1\right)}} + ..., \tag{64}$$

where the dots denote terms that are subleading as $r_* \to r_0$. This way we get

$$S = \Delta r_0 |\mathbf{x}-\mathbf{x}'| + ... \tag{65}$$

where the dots denote terms that increase slower than linearly in the limit of large $|\mathbf{x}-\mathbf{x}'|$. Using (58) we obtain

$$G(\mathbf{x},\mathbf{x}') = \langle \mathcal{O}(\mathbf{x},t)\mathcal{O}(\mathbf{x}',t)\rangle \propto e^{-|\mathbf{x}-\mathbf{x}'|/\xi}, \tag{66}$$

where the correlation length is given by

$$\xi = \frac{1}{\Delta r_0}. \tag{67}$$

In order to obtain the temperature dependence of the correlation length we need to know the relation between the temperature and the position of the horizon. This has to be obtained mostly numerically. The temperature is related to the position of the horizon through (49), keeping ρ in (52) fixed. Figure 4 shows the results of a numerical evaluation of (67) for both holographic models as a function of $T/\rho^{z/2}$. A numerical evaluation of the full correlation function in the geodesic approximation for $z = 2$ is shown in Figure 5. Correlation functions for other values of z and different values of $T/\rho^{z/2}$ are qualitatively very similar to the ones shown in the figure. As can be seen from Figure 5, the numerical solution indeed agrees with our (approximate) analytic result (67) at large distances.

The short distance behavior of the correlation function has the form

$$G(\mathbf{x},\mathbf{x}') \approx \frac{1}{|\mathbf{x}-\mathbf{x}'|^{2\Delta}}, \tag{68}$$

---

[6] The integral in (62) is also divergent at the upper limit when the cutoff is sent to zero. This divergence is independent of r_* and has the same value in the vacuum. We can ignore it as it cancels with the explicit power of ϵ in (58).

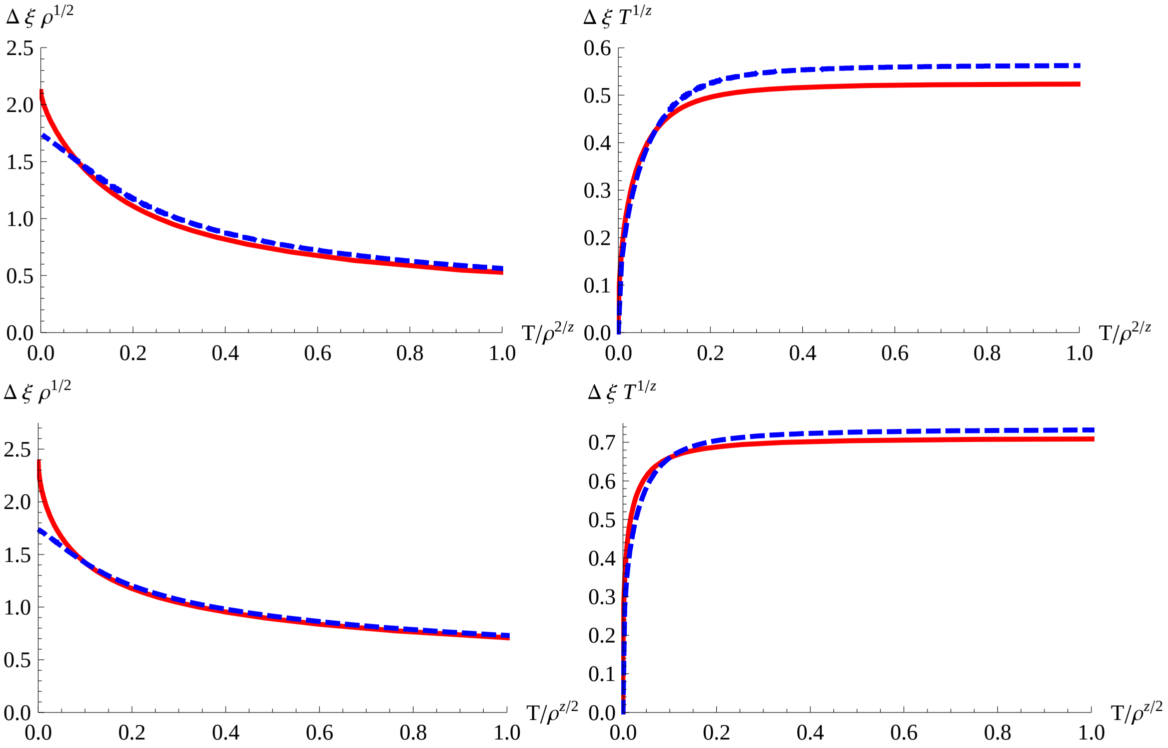

Figure 4: Correlation lengths in the two models as a function of $T/\rho^{2/z}$ for the dynamical critical exponent $z = 2$ (top) and $z = 3$ (bottom). The solid red curves correspond to the EMP model and the dashed blue curve corresponds to the EDM model.

independently of the temperature.

As can be seen from Figure 4, the correlation length approaches a finite non-vanishing constant value as $T \to 0$ while keeping the charge density fixed. For a vanishing chemical potential the correlation length diverges as $\xi \propto T^{-1/z}$ as Figure 4 indicates.

5.2 General scaling dimensions

When the scaling dimensions of the operators in the two point function are small, the geodesic approximation no longer applies and one has to solve the full wave-equation. The Euclidean action for the boson is taken to have the standard form[7]

$$S_E = \frac{1}{2}\int d^4x\sqrt{-g}\Big((\partial\phi)^2 + m^2\phi^2\Big) + \frac{1}{2}\Delta_-\int d^3x\sqrt{-\gamma}\phi^2|_{r=\epsilon^{-1}}, \qquad (69)$$

---

[7] We note that the counter term in (69) is not the most general one, but it applies to the values of the scaling dimension $\Delta < 2 + z/2$, to which we specialize in what follows. More generally one has terms including derivatives with respect to the transverse dimensions [9].

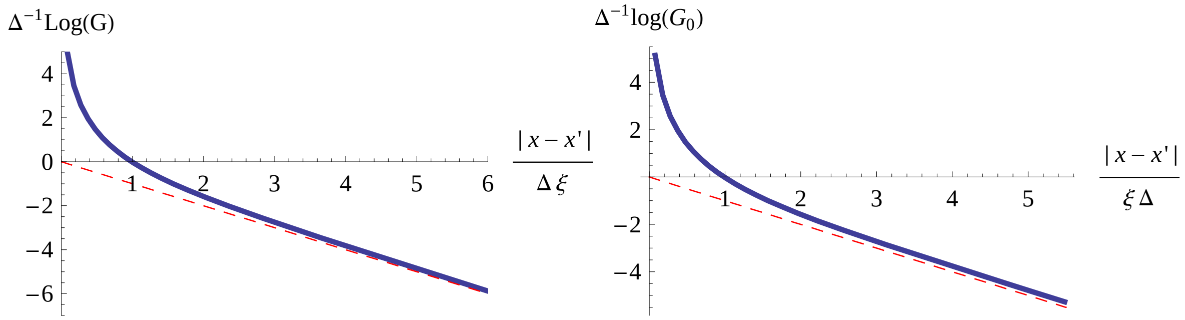

Figure 5: Logarithm of the two point equal time correlation function as a function of distance for $z = 2$. The dashed line corresponds to a reference line with slope -1. The left figure is in the EDM model and $T/\rho^{z/2} \approx 0.0229$ while the right figure is in the EMP model with $T/\rho^{z/2} \approx 0.109$. Correlators for other temperature values are almost indistinguishable from the ones shown in the figure. Most of the dependence on z and T comes through ξ.

where γ is the determinant of the induced metric at $r = \epsilon^{-1}$ and Δ_- is given below equation (75). The two point function is obtained by solving the wave equation,

$$\frac{1}{\sqrt{-g}}\partial_\mu(\sqrt{-g}g^{\mu\nu}\partial_\nu\phi) - m^2\phi = 0, \tag{70}$$

in the bulk spacetime. We are interested in correlation functions at thermal equilibrium, and thus we work in Euclidean signature. This means in particular that the field ϕ should be Fourier transformed as

$$\phi(\mathbf{x}, r, \tau) = \sum_n \int \frac{d^2k}{(2\pi)^2} e^{-i\omega_n\tau + i\mathbf{k}\cdot\mathbf{x}}\phi_n(r, k), \tag{71}$$

where $\omega_n = 2\pi T n$ are the Matsubara mode frequencies. To obtain the bulk to boundary propagator we require regularity at the horizon. For the numerics we find it convenient to use the coordinate $u = 1/r$ in terms of which the metric reads

$$ds^2 = f(u)\frac{d\tau^2}{u^{2z}} + \frac{1}{u^2}\Big(\frac{du^2}{g(u)} + d\mathbf{x}^2\Big). \tag{72}$$

We are lead to solve the wave equation

$$u^{3+z}\sqrt{\frac{g}{f}}\partial_u(u^{-1-z}\sqrt{fg}\partial_u\phi_n) - \Big(\frac{u^{2z}}{f}\omega_n^2 + u^2k^2 + m^2\Big)\phi_n = 0, \tag{73}$$

together with the regularity condition, that, close to the horizon $u = u_0 \equiv 1/r_0$, the field behaves as

$$\phi_n(u, k) \approx \phi_n^{(0)} \exp\left[-u_0^{z-1}\omega_n \int^u \frac{du'}{\sqrt{f(u')g(u')}}\right], \tag{74}$$

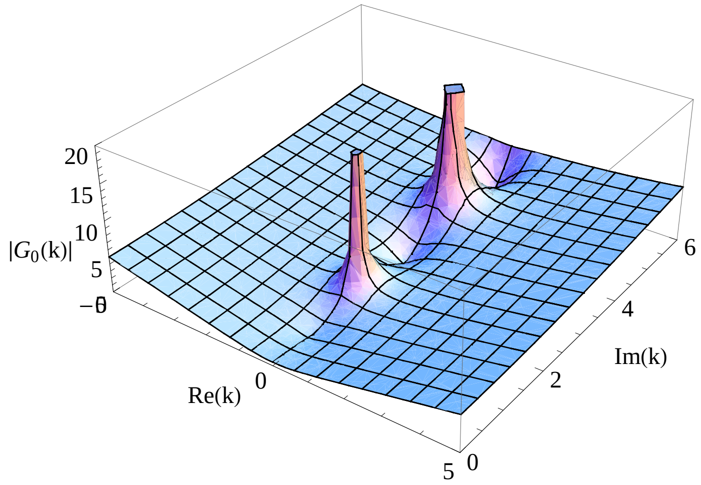

Figure 6: The momentum space correlator for $z = 2$ and $\omega_n = 0$ in the EMD model at finite temperature and zero charge density. The scaling dimension of the scalar operator is $\Delta = 2 + \sqrt{3}/2$.

where $\phi_n^{(0)}$ has a regular Taylor expansion in $u - u_0$. The modes $\phi_n(u, k)$ have the standard asymptotic behavior as $u \to 0$

$$\phi_n(u, k) = \phi_n^{(-)} u^{\Delta_-} + \phi_n^{(+)} u^{\Delta_+} + ..., \tag{75}$$

where $\Delta_\pm = (2 + z)/2 \pm \nu$ and $\nu = \sqrt{(2 + z)^2/4 + m^2}$. The holographic dictionary with our Fourier transform conventions reads

$$e^{-S_E} = \left\langle \exp\left[\beta \sum_n \int \frac{d^2k}{(2\pi)^2} \mathcal{O}_n(k) \phi_{-n}^{(-)}(-k)\right]\right\rangle, \tag{76}$$

which leads to the two point function

$$\begin{aligned} \langle \mathcal{O}_n(k) \mathcal{O}_{n'}(k') \rangle &= -\frac{(2\pi)^4}{\beta^2} \frac{\delta^2 S_E}{\delta\phi_{-n}^{(-)}(-k)\delta\phi_{-n'}^{(-)}(-k')} \\ &= T\delta_{n+n',0}\delta^2(k + k')(2\pi)^2 G_n(k), \end{aligned} \tag{77}$$

where

$$G_n(k) = 2\nu \frac{\phi_n^{(+)}}{\phi_n^{(-)}}. \tag{78}$$

For the alternative quantization [39,40] (which corresponds to treating the subleading mode $\phi^{(+)}$ as the source) we have

$$G_n(k) = -(2\nu)^{-1} \frac{\phi_n^{(-)}}{\phi_n^{(+)}}. \tag{79}$$

The momentum space correlator has poles on the imaginary k axis, which means that the real space two point function decays exponentially, $G(\mathbf{x},\mathbf{x}') \propto e^{-k_*|\mathbf{x}-\mathbf{x}'|}$, where k_* is the pole closest to the real k axis. It is sufficient to take into account the lowest Matsubara mode as the higher ones have a faster fall of in position space[8]. We solve (73) numerically and extract the momentum space two point correlator using (78), with $n = 0$. Results from a numerical evaluation of the finite temperature two point correlator is shown in Figure 6. This indeed shows poles on the imaginary k axis.

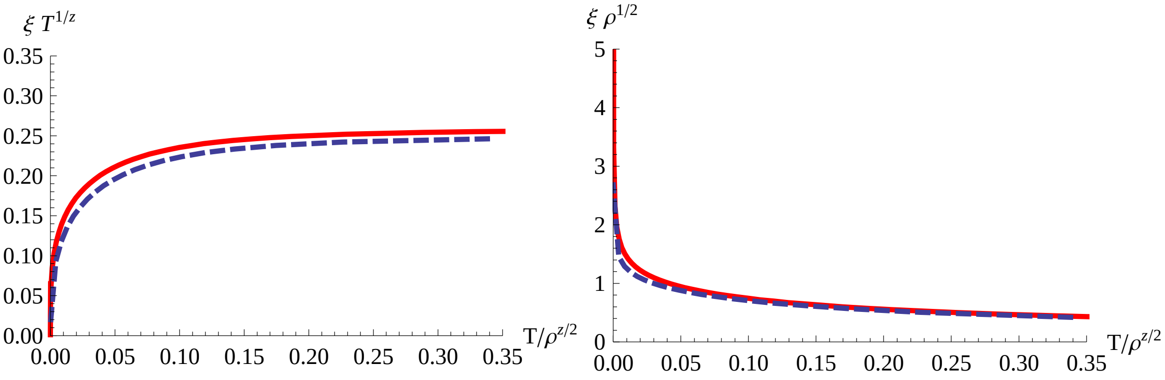

Figure 7: The correlation length, as extracted from the position of the lowest pole of the momentum space correlator, as a function of $T/\rho^{z/2}$. The dashed (blue) curves are in the EMD model while the solid (red) curves are in the EMP model. All the plots are for $z = 2$ and $\Delta = 2 + \sqrt{3}/2$.

By tracking the position of the lowest pole in the momentum space propagator, we can obtain the correlation length as a function of $T/\rho^{z/2}$ as the temperature is varied. The correlation length for $z = 2$ obtained this way is shown in Figure 7 for both holographic models.

6 Double trace deformations

In the previous section we considered the finite temperature dependence of scalar correlation functions at finite charge density. While working at finite charge density gives rise to non-trivial dependence on the dimensionless ratio of the length scales associated to ρ and T, it has the drawback that at zero temperature there is still a finite length scale in the problem, associated with the charge density.

Another way to study the temperature dependence of the correlation length is to work at zero charge density and add a double trace deformation for the scalar operator [42, 43],

---

[8] The same procedure has been used earlier in calculating the Debye screening length using holography in $\mathcal{N} = 2^*$ supersymmetric Yang-Mills theory [41].

$$\delta S_E = \frac{1}{2}\int d^3x \lambda \mathcal{O}(x)^2. \tag{80}$$

The coupling constant λ introduces a new reference length scale into the problem, which, when combined with T, gives rise to a dimensionless ratio that enters into thermal correlators. For a concise review of double trace deformations see the Appendix of [44].

A prescription for calculating two point correlation functions in AdS/CFT in the presence of a double trace deformation was given in [45]. The same argument goes through in asymptotically Lifshitz spacetime and we do not repeat it here. Denoting the original momentum space two point function as $G_n(k)$, the two point function in the deformed theory is found to be

$$G_n^{(\lambda)}(k) = \frac{G_n(k)}{1+\lambda G_n(k)}. \tag{81}$$

The form of the two point function (81) can also be understood in a simple way from large-N factorization of correlation functions. The deformed two point function is

$$\left\langle \mathcal{O}_n(k)\mathcal{O}_{n'}(k')e^{-\frac{1}{2}\beta\sum_n\int\frac{d^2q}{(2\pi)^2}\lambda\mathcal{O}_n(q)\mathcal{O}_{-n}(-q)}\right\rangle = T\delta_{n+n',0}\delta^2(k+k')(2\pi)^2G_n^{(\lambda)}(k), \tag{82}$$

which after expanding the exponential in a power series, and using large-N factorization, becomes

$$G_n^{(\lambda)}(k) = \sum_{m=1}^{\infty} G_n(k)^m\lambda^{m-1} = \frac{G_n(k)}{1+\lambda G_n(k)}, \tag{83}$$

recovering (81).

The method that was described in the previous section for solving for the two point function $G(k)$ applies here as well. Since we are interested in relevant deformations of the theory, we consider correlation functions in the alternative quantization [39, 40], for which the undeformed correlator is given by (79). In this case the deformed correlator becomes

$$G_n^{(\lambda)}(k) = \left(\lambda - 2\nu\frac{\phi_n^{(+)}(k)}{\phi_n^{(-)}(k)}\right)^{-1}. \tag{84}$$

By tracking the lowest pole of the deformed two point function (84) we obtain the correlation length shown in Figure 8. At high temperature the dimensionless correlation length $\xi T^{1/2}$ is simply that of the alternative quantization without a double trace deformation. As the temperature is lowered, the dimensionless combination $\xi T^{1/2}$ flows from its value in the alternative quantization, to its value in the standard quantization. This reflects the renormalization group flow from the alternative quantization to the standard one [40, 44]. In the vacuum the renormalization group flow is seen when considering the behavior of the correlation function as a function

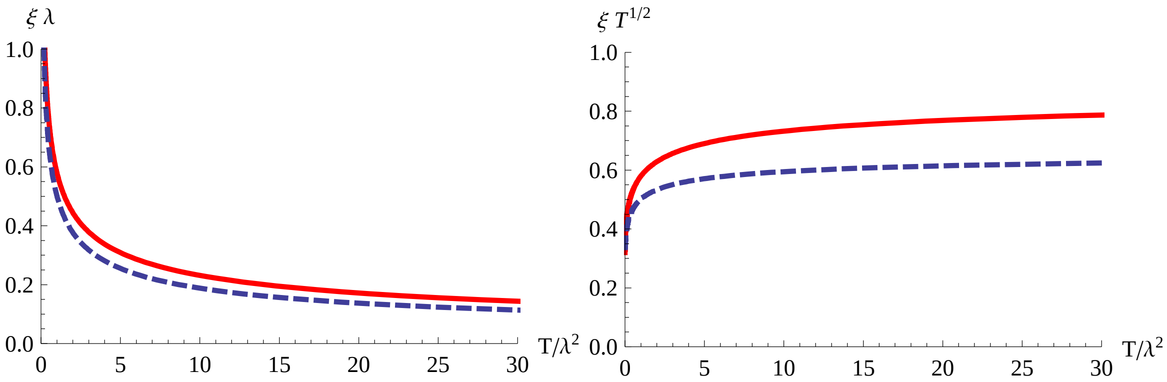

Figure 8: The correlation length as extracted from the position of the lowest pole of the momentum space correlator in the double trace deformed theory. The solid red curves are in the EMP theory while the dashed blue curves are in the EDM theory. Both plots are for $z = 2$ and $\Delta = 3/2$.

of distance, short distances corresponding to the alternative quantization and large distances to the standard quantization. In our case the renormalization group flow is instead revealed as a function of the temperature.

7 Discussion

In this paper we have considered two bottom up holographic models both of which admit a metric with a Lifshitz scaling symmetry, with arbitrary dynamical critical exponent, and include a $U(1)$ gauge field. Both models have charged black brane solutions that give access to finite temperature physics in the corresponding dual field theories. At high temperature (compared to the scale set the $U(1)$ charge density) the behavior of thermodynamic quantities is governed by the underlying Lifshitz scaling symmetry. As the temperature is lowered, keeping the charge density fixed, various thermodynamic quantities in the two models start to differ from each other. In particular, a sharp distinction between the two models appears in the specific heat, which for the EMD model behaves at low temperatures as

$$\frac{C}{T} \to \text{const.} \quad \text{as} \quad T \to 0, \tag{85}$$

while numerical results suggest that C/T grows without bound in the limit of zero temperature in the EMP model [34]. It thus appears that the same relevant deformation, by a chemical potential, takes us to a different kind of a fixed point in the zero temperature limit in the two models, at least as far as thermodynamics is concerned. The infrared (near horizon) geometry of extremal black branes has an $\mathrm{AdS}_2 \times \mathrm{R}^2$

region in both of the models, as discussed in section 3, but in the EMP model only after a singular coordinate transformation.

For the finite temperature equal time two point function, at finite charge density, we find the standard power law behavior at short distances, while for large distances it decays exponentially due to the presence of a horizon in the bulk. The correlation length extracted from the exponential decay is shown in Figure 4 for large scaling dimension operators and in Figure 7 for generic scaling dimensions. For high temperatures $T/\rho^{z/2} > 0.2$, the temperature dependence of the correlation length is consistent with scale invariance, implying a large temperature range where the critical point dominates the physics. As expected, the two models agree quite well in this range. On the other hand, the correlation length exhibits distinctly different behavior in the two models at low temperature and fixed charge density. In the EMD model we obtain the following behavior in the geodesic approximation,

$$\left(\frac{\partial\xi}{\partial T}\right)_\rho \to \text{const.}, \tag{86}$$

while the same quantity diverges in the zero temperature limit in the EMP model,

$$\left(\frac{\partial\xi}{\partial T}\right)_\rho \to -\infty. \tag{87}$$

In both cases ξ tends to a finite value as $T \to 0$ when the charge density is kept fixed at a non-zero value.

The correlation length in the presence of a double trace deformation is shown in Figure 8. In this case the correlation length diverges in both models in the zero temperature limit, while keeping the double trace coupling λ fixed. The temperature dependence of the correlation length has a scale invariant form in two regions, at high temperatures and at low temperatures. The combination $\xi T^{1/z}$ runs between its fixed point values, from the alternative quantization at high temperatures to the standard quantization at low temperatures. Overall, the double trace deformation leads to a qualitatively very similar behavior in both holographic models.

The double trace deformation leads to a Lifshitz symmetric result in the zero temperature limit while at fixed charge density there remains a finite length scale in the problem even at zero temperature. We can therefore more meaningfully compare the double trace deformation case to the quantum Lifshitz model, which, as was reviewed in section 2, has several temperature dependent length scales. The scale associated with a vortex plasma in the quantum Lifshitz model behaves as $\xi_{vortex} \propto e^{-E_c/2T}$, which changes more rapidly with T than we find in the holographic correlation functions. The comparison to the "intermediate" length scale ξ_T in (14), given by

$$\xi_T T^{1/2} \propto \sqrt{\frac{\log(-\log T)}{-\log T}}, \tag{88}$$

works somewhat better. The dimensionless combination $\xi_T T^{1/2}$ is seen to be a fairly mild function of temperature, even if it diverges in the zero temperature limit. At a qualitative level, the double trace deformation gives rise to similar behavior as it induces a mild temperature dependence on $\xi T^{1/z}$.

Both types of deformations in both holographic models show similar behavior for the combination $\xi T^{1/z}$. It is seen to be an increasing function of temperature in all of the cases we have studied here. It would be interesting to understand this from the perspective of the finite temperature renormalization group.

8 Acknowledgements

This work was supported in part by the Icelandic Research Fund and by the University of Iceland Research Fund. We would like to thank Tobias Zingg and Sean Nowling for discussions.

References

[1] S. A. Hartnoll, "Lectures on holographic methods for condensed matter physics," Class. Quant. Grav. **26**, 224002 (2009) [arXiv:0903.3246 [hep-th]].

[2] C. P. Herzog, "Lectures on Holographic Superfluidity and Superconductivity," J. Phys. A **42**, 343001 (2009) [arXiv:0904.1975 [hep-th]].

[3] G. T. Horowitz, "Introduction to Holographic Superconductors," arXiv:1002.1722 [hep-th].

[4] J. McGreevy, "Holographic duality with a view toward many-body physics," Adv. High Energy Phys. **2010**, 723105 (2010) [arXiv:0909.0518 [hep-th]].

[5] S. Sachdev, "Condensed matter and AdS/CFT," arXiv:1002.2947 [hep-th].

[6] S. Sachdev, "Quantum phase transitions," Cambridge U. Press (2000).

[7] S. L. Sondhi, S. M. Girvin, J. P. Carini, D. Shahar "Continuous quantum phase transitions," Rev. Mod. Phys. **69**, (1997) 315333. [cond-mat/9609279].

[8] S. Kachru, X. Liu, and M. Mulligan, "Gravity Duals of Lifshitz-like Fixed Points," Phys. Rev. D **78** (2008) 106005 [arXiv:0808.1725 [hep-th]].

[9] M. Taylor, "Non-relativistic holography," arXiv:0812.0530 [hep-th].

[10] E. J. Brynjolfsson, U. H. Danielsson, L. Thorlacius and T. Zingg, "Holographic Superconductors with Lifshitz Scaling," J. Phys. A A **43**, 065401 (2010) [arXiv:0908.2611 [hep-th]].

[11] J. Tarrio and S. Vandoren, "Black holes and black branes in Lifshitz spacetimes," JHEP **1109**, 017 (2011) [arXiv:1105.6335 [hep-th]].

[12] A. Viswanath, L. Balents, T. Senthil, "Quantum criticality and deconfinement in phase transitions between valence bond solids," Phys. Rev. **B69** (2004) 224416. [cond-mat/0311085].

[13] E. Fradkin, D. A. Huse, R. Moessner, V. Oganesyan, S. L. Sondhi, "Bipartite RokhsarKivelson points and Cantor deconfinement," Phys. Rev. **B69** (2004) 224415. [cond-mat/0311353].

[14] E. Ardonne, P. Fendley, E. Fradkin, "Topological Order and Conformal Quantum Critical Points," Ann. Phys. (N.Y.) **310** (2004) 493. [cond-mat/0311466].

[15] P. Ghaemi, A. Vishwanath, T. Senthil, "Finite-temperature properties of quantum Lifshitz transitions between valence-bond solid phases: An example of local quantum criticality," Phys. Rev. **B72** (2005) 024420. [cond-mat/0412409].

[16] P. Koroteev, M. Libanov, "On Existence of Self-Tuning Solutions in Static Braneworlds without Singularities," JHEP **0802**, 104 (2008). [arXiv:0712.1136 [hep-th]].

[17] E. J. Brynjolfsson, U. H. Danielsson, L. Thorlacius and T. Zingg, "Holographic Models with Anisotropic Scaling," arXiv:1004.5566 [hep-th].

[18] D. -W. Pang, "On Charged Lifshitz Black Holes," JHEP **1001**, 116 (2010) [arXiv:0911.2777 [hep-th]].

[19] U. H. Danielsson and L. Thorlacius, "Black holes in asymptotically Lifshitz spacetime," JHEP **0903**, 070 (2009) [arXiv:0812.5088 [hep-th]].

[20] V. Keranen, E. Keski-Vakkuri and L. Thorlacius, "Thermalization and entanglement following a non-relativistic holographic quench," Phys. Rev. D **85**, 026005 (2012) [arXiv:1110.5035 [hep-th]].

[21] G. Bertoldi, B. A. Burrington and A. Peet, "Black Holes in asymptotically Lifshitz spacetimes with arbitrary critical exponent," Phys. Rev. D **80**, 126003 (2009) [arXiv:0905.3183 [hep-th]].

[22] S. F. Ross and O. Saremi, "Holographic stress tensor for non-relativistic theories," JHEP **0909**, 009 (2009) [arXiv:0907.1846 [hep-th]].

[23] T. Zingg, "Thermodynamics of Dyonic Lifshitz Black Holes," JHEP **1109**, 067 (2011) [arXiv:1107.3117 [hep-th]].

[24] S. F. Ross, "Holography for asymptotically locally Lifshitz spacetimes," Class. Quant. Grav. **28**, 215019 (2011) [arXiv:1107.4451 [hep-th]].

[25] M. Baggio, J. de Boer and K. Holsheimer, "Hamilton-Jacobi Renormalization for Lifshitz Spacetime," JHEP **1201** (2012) 058 [arXiv:1107.5562 [hep-th]].

[26] R. B. Mann and R. McNees, "Holographic Renormalization for Asymptotically Lifshitz Spacetimes," JHEP **1110**, 129 (2011) [arXiv:1107.5792 [hep-th]].

[27] J. Tarrio, "Asymptotically Lifshitz Black Holes in Einstein-Maxwell-Dilaton Theories," arXiv:1201.5480 [hep-th].

[28] M. Cubrovic, J. Zaanen and K. Schalm, "String Theory, Quantum Phase Transitions and the Emergent Fermi-Liquid," Science **325** (2009) 439 [arXiv:0904.1993 [hep-th]].

[29] H. Liu, J. McGreevy and D. Vegh, "Non-Fermi liquids from holography," Phys. Rev. D **83** (2011) 065029 [arXiv:0903.2477 [hep-th]].

[30] T. Faulkner, H. Liu, J. McGreevy and D. Vegh, "Emergent quantum criticality, Fermi surfaces, and AdS(2)," Phys. Rev. D **83** (2011) 125002 [arXiv:0907.2694 [hep-th]].

[31] U. Gursoy, E. Plauschinn, H. Stoof and S. Vandoren, "Holography and ARPES Sum-Rules," arXiv:1112.5074 [hep-th].

[32] L. Q. Fang, X. -H. Ge and X. -M. Kuang, "Holographic fermions in charged Lifshitz theory," arXiv:1201.3832 [hep-th].

[33] M. Alishahiha, M. R. Mohammadi Mozaffar and A. Mollabashi, "Fermions on Lifshitz Background," arXiv:1201.1764 [hep-th].

[34] E. J. Brynjolfsson, U. H. Danielsson, L. Thorlacius and T. Zingg, "Black Hole Thermodynamics and Heavy Fermion Metals," JHEP **1008** (2010) 027 [arXiv:1003.5361 [hep-th]].

[35] G. Bertoldi, B. A. Burrington and A. W. Peet, "Thermodynamics of black branes in asymptotically Lifshitz spacetimes," Phys. Rev. D **80**, 126004 (2009) [arXiv:0907.4755 [hep-th]].

[36] K. Balasubramanian and J. McGreevy, "An Analytic Lifshitz black hole," Phys. Rev. D **80** (2009) 104039 [arXiv:0909.0263 [hep-th]].

[37] A. Giacomini, G. Giribet, M. Leston, J. Oliva and S. Ray, "Scalar field perturbations in asymptotically Lifshitz black holes," arXiv:1203.0582 [hep-th].

[38] V. Balasubramanian, S. F. Ross, “Holographic particle detection,” Phys. Rev. **D61** (2000) 044007. [hep-th/9906226].

[39] V. Balasubramanian, P. Kraus and A. E. Lawrence, “Bulk versus boundary dynamics in anti-de Sitter space-time,” Phys. Rev. D **59** (1999) 046003 [hep-th/9805171].

[40] I. R. Klebanov and E. Witten, “AdS / CFT correspondence and symmetry breaking,” Nucl. Phys. B **556** (1999) 89 [hep-th/9905104].

[41] C. Hoyos, S. Paik and L. G. Yaffe, “Screening in strongly coupled N=2* supersymmetric Yang-Mills plasma,” JHEP **1110** (2011) 062 [arXiv:1108.2053 [hep-th]].

[42] M. Berkooz, A. Sever and A. Shomer, “’Double trace’ deformations, boundary conditions and space-time singularities,” JHEP **0205** (2002) 034 [hep-th/0112264].

[43] E. Witten, “Multitrace operators, boundary conditions, and AdS / CFT correspondence,” hep-th/0112258.

[44] T. Faulkner, H. Liu and M. Rangamani, “Integrating out geometry: Holographic Wilsonian RG and the membrane paradigm,” JHEP **1108** (2011) 051 [arXiv:1010.4036 [hep-th]].

[45] W. Mueck, “An Improved correspondence formula for AdS / CFT with multitrace operators,” Phys. Lett. B **531** (2002) 301 [hep-th/0201100].